

# Longitudinal Spin Transfer to the $\Lambda$ and $\bar{\Lambda}$ Hyperons in Muon-Nucleon Deep-Inelastic Scattering

M.G.Sapozhnikov

On behalf of the COMPASS Collaboration

Joint Institute for Nuclear Research, Laboratory of High Energy Physics  
Dubna, Russia

The longitudinal polarisation transfer from muons to  $\Lambda$  and  $\bar{\Lambda}$  hyperons,  $D_{LL}^{\Lambda(\bar{\Lambda})}$ , has been studied in deep inelastic scattering off an unpolarised isoscalar target at the COMPASS experiment at CERN. The spin transfers to  $\Lambda$  and  $\bar{\Lambda}$  produced in the current fragmentation region exhibit different behaviours as a function of  $x$  and  $x_F$ . The measured  $x$  and  $x_F$  dependences of  $D_{LL}^{\Lambda}$  are compatible with zero, while  $D_{LL}^{\bar{\Lambda}}$  tends to increase with  $x_F$ .

## 1 Introduction

The study of the  $\Lambda$  and  $\bar{\Lambda}$  hyperon polarisation in DIS is important for the understanding of the nucleon structure, the mechanisms of hyperon production and the hyperon spin structure. In particular, it may provide valuable information on the unpolarised strange quark distributions  $s(x)$  and  $\bar{s}(x)$  in the nucleon.

We have studied  $\Lambda$  and  $\bar{\Lambda}$  production by scattering 160 GeV polarised  $\mu^+$  off a polarised  ${}^6\text{LiD}$  target in the COMPASS experiment (NA58) at CERN. A detailed description of the COMPASS experimental setup is given elsewhere [2].

The data used in the present analysis were collected during the years 2003-2004. The longitudinally polarised muon beam has an average polarisation of  $P_b = -0.76 \pm 0.04$  in the 2003 run and of  $P_b = -0.80 \pm 0.04$  in the 2004 run. The target consists of two 60 cm long, oppositely polarised cells. Typical polarization values of 50% are obtained by dynamic nuclear polarization, and measured with a relative accuracy of 5%. The dilution factor  $f$  is about 40%. The data from both longitudinal target spin orientations were recorded simultaneously.

The event selection requires a reconstructed interaction vertex defined by the incoming and the scattered muon located inside the target. DIS events are selected by cuts on the photon virtuality ( $Q^2 > 1 \text{ (GeV}/c)^2$ ) and on the fractional energy of the virtual photon ( $0.2 < y < 0.9$ ). The  $\Lambda$  and  $\bar{\Lambda}$  hyperons are identified by their decays into  $p\pi^-$  and  $\bar{p}\pi^+$ . In order to suppress background events, the secondary vertex is required to be within a 105 cm long fiducial region starting 5 cm downstream of the target. The angle  $\theta_{col}$  between the hyperon momentum and the line connecting the primary and the secondary vertex is required to be  $\theta_{col} < 0.01$  rad. This cut selects events with the correct direction of the hyperon momentum vector with respect to the primary vertex, which results in a reduction of the combinatorial background. A cut on the transverse momentum  $p_t$  of the decay products with respect to the hyperon direction of  $p_t > 23 \text{ MeV}/c$  is applied to reject  $e^+e^-$  pairs due to  $\gamma$  conversion. Only particles with momenta larger than 1 GeV/c were selected to provide optimal tracking efficiency.

The main sources of background are events from  $K_S^0$  decays and combinatorial background. A Monte Carlo (MC) simulation shows that the percentage of kaon background

changes from 1 to 20 %, when  $\cos\theta$  varies from -1 to 1, where  $\theta$  is the angle between the direction of the decay proton(antiproton) in the  $\Lambda(\bar{\Lambda})$  rest frame and the quantization axis along the momentum vector of the virtual photon. At small and negative values of  $\cos\theta$  the invariant mass distribution of the kaon background is flat. However, at  $\cos\theta \sim 1$ , the kaon contribution is concentrated mainly at small values of the invariant mass on the left side of the  $\Lambda(\bar{\Lambda})$  peak. In this angular region the distribution of the kaon events under the  $\Lambda(\bar{\Lambda})$  peak changes rapidly. In order to minimize the influence of the kaon background, the angular interval was limited to  $-1 < \cos\theta < 0.6$ . This cut reduces the  $\Lambda(\bar{\Lambda})$  signal by  $\sim 10\%$ . The total number of events after all cuts is  $N(\Lambda) = 69500 \pm 360$ ,  $N(\bar{\Lambda}) = 41600 \pm 310$  and  $N(K_S^0) = 496000 \pm 830$ . The large amount of  $\bar{\Lambda}$  events is a unique feature of the COMPASS experiment.

## 2 Experimental results

After correcting for the apparatus acceptance, the angular distribution of the decay protons(antiprotons) in the  $\Lambda(\bar{\Lambda})$  rest frame is

$$\frac{1}{N_{tot}} \cdot \frac{dN}{d\cos\theta} = \frac{1}{2} \cdot (1 + \alpha P_L \cos\theta). \quad (1)$$

Here,  $N_{tot}$  is the total number of  $\Lambda(\bar{\Lambda})$ , the longitudinal polarization  $P_L$  is the projection of the polarisation vector on the momentum vector of the virtual photon,  $\alpha = +(-)0.642 \pm 0.013$  is the  $\Lambda(\bar{\Lambda})$  decay parameter,  $\theta$  is the angle between the direction of the decay proton for  $\Lambda$  (antiproton - for  $\bar{\Lambda}$ , positive  $\pi$  - for  $K_S^0$ ) and the corresponding axis. The acceptance correction was determined using the MC simulation for unpolarised  $\Lambda$  and  $\bar{\Lambda}$  decays. The angular dependence of the acceptance is quite smooth, it decreases by a factor 1.2-1.3 in the angular range of the measurement.

To determine the  $\Lambda(\bar{\Lambda})$  angular distributions, a sideband subtraction method is used. The events with an invariant mass within a  $\pm 1.5 \sigma$  interval from the mean value of the  $\Lambda(\bar{\Lambda})$  peak are taken as signal. The background regions are selected from the left and right sides of the invariant mass peak. Each band is  $2 \sigma$  wide and starts at a distance of  $3 \sigma$  from the central value of the peak. The  $\Lambda(\bar{\Lambda})$  angular distribution is determined by subtracting the averaged angular distribution of the events in the sidebands from the angular distribution of those in the signal region. The longitudinal polarisation  $P_L$  is then obtained from a fit of the angular distribution (1).

It was found that the polarization of the hyperons weakly depends on the polarization of the target. The polarization difference  $\Delta P = P_- - P_+$  between the  $\Lambda(\bar{\Lambda})$  polarization for negative target polarization (anti-parallel to the beam muon spin) and positive (parallel to the beam muon spin) target polarization is compatible with zero within the statistical errors.

$$\Delta P(\Lambda) = -0.01 \pm 0.04, \quad (2)$$

$$\Delta P(\bar{\Lambda}) = 0.01 \pm 0.05. \quad (3)$$

In Fig. 1 it is shown that for  $\Lambda$  the polarization difference is  $\Delta P \sim 0$  for all  $x$  region, whereas for  $\bar{\Lambda}$  the  $\Delta P$  seems change its sign. For the further analysis the data from both target spin orientations were averaged.

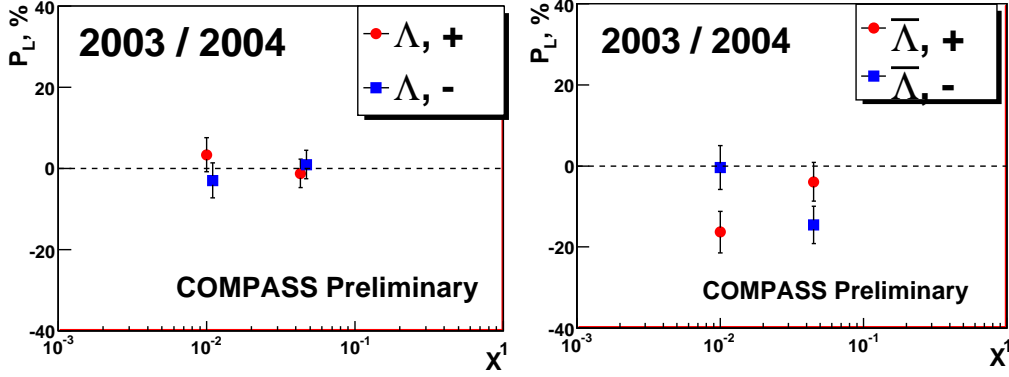


Figure 1: The  $x$  dependence of the longitudinal polarization of  $\Lambda$  and  $\bar{\Lambda}$  hyperons for different target polarization.

To compare results of different experiments, it is worthwhile to use the longitudinal spin transfer  $D_{LL}^{\Lambda}$ , which relates the longitudinal polarisation of the hyperon  $P_L$  to the polarisation of the incoming lepton beam  $P_b$ :

$$P_L = D_{LL}^{\Lambda} \cdot P_b \cdot D(y), \quad (4)$$

where  $D(y)$  is the virtual photon depolarization factor given by:

$$D(y) = \frac{1 - (1 - y)^2}{1 + (1 - y)^2}. \quad (5)$$

To evaluate the spin transfer, the product  $P_b \cdot D(y)$  is calculated for each event passing the selection criteria. The beam polarization  $P_b$  is parametrised as a function of the incident muon momentum [2].

The weighted averages of the spin transfers for the 2003 and the 2004 data are:

$$D_{LL}^{\Lambda} = -0.012 \pm 0.047(stat) \pm 0.024(sys), \quad \bar{x}_F = 0.22, \quad (6)$$

$$D_{LL}^{\bar{\Lambda}} = 0.249 \pm 0.056(stat) \pm 0.049(sys), \quad \bar{x}_F = 0.20. \quad (7)$$

The systematic errors are mainly due to the uncertainty on the acceptance corrections determined by the Monte Carlo simulation. The presence of other systematic effects was checked by looking at a physical process with no polarization effects, i.e. the longitudinal spin transfers to the  $K_S^0$ , and by checking the stability of the result while varying the selection cuts. The longitudinal spin transfer to the  $K_S^0$  turns out to be  $D_{LL}^{K_S^0} = 0.016 \pm 0.010$  and is taken as an estimate for the corresponding systematic error  $\delta(K_S^0)$ . Some systematic effect  $\delta(\theta)$  appears due to variation of the cut on  $\cos\theta$ . The uncertainty of the sidebands subtraction method,  $\delta(ss)$  is estimated by varying the width of the signal band from  $\pm 1.5\sigma$  to  $\pm 1$ ,  $\pm 1.25$ ,  $\pm 1.75$  and  $\pm 2\sigma$ . Another source of systematic errors is the uncertainty in the beam polarisation,  $\delta(P_b)$ . The relative error in the value of beam polarisation is 0.05.

The  $x$  and  $x_F$  dependences of the spin transfers to  $\Lambda$  and  $\bar{\Lambda}$  are shown in Fig. 2. One could see that these dependences are different for  $\Lambda$  and  $\bar{\Lambda}$ . The spin transfer to  $\Lambda$  is small and compatible with zero, while the spin transfer to  $\bar{\Lambda}$  may reach values as large as  $D_{LL}^{\bar{\Lambda}} = 0.4 - 0.5$ .

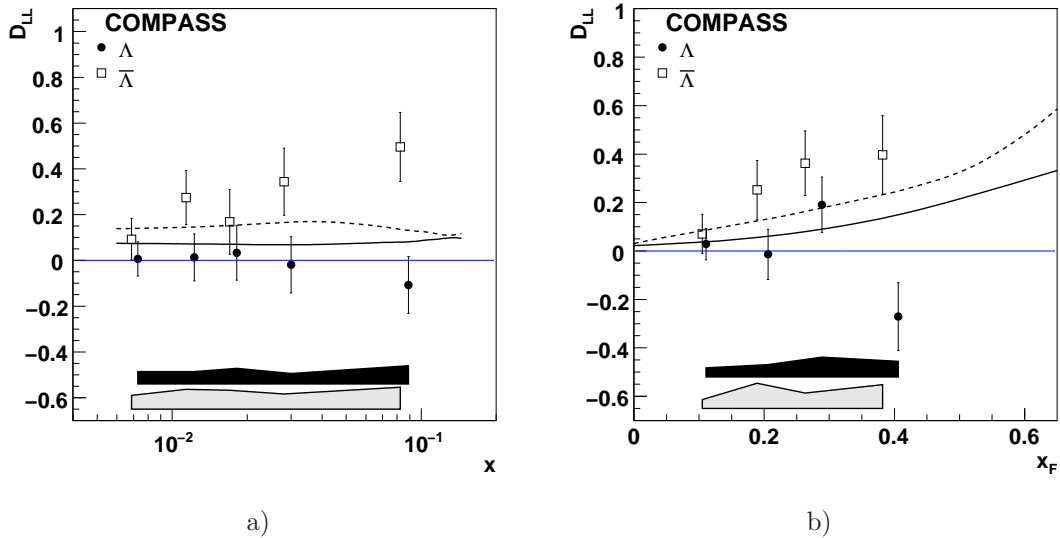


Figure 2: The  $x$  (a) and  $x_F$  (b) dependence of the longitudinal spin transfer to  $\Lambda$  and  $\bar{\Lambda}$ . The solid line corresponds to the theoretical calculations of [3] for  $\Lambda$  and the dashed line is for the  $\bar{\Lambda}$  spin transfer. The black(shaded) bands give the size of the systematic errors for  $\Lambda(\bar{\Lambda})$ .

### 3 Discussion

Figure 2 shows that indeed calculations of the model [3] lead to a larger spin transfer to  $\bar{\Lambda}$  than to  $\Lambda$ . The same trend was found in the recent calculation of [4]. The model [3] predicts that the contribution from the strange quarks (antiquarks) is essential for the spin transfer to  $\Lambda(\bar{\Lambda})$ . In Fig. 3 the degree of the sensitivity to the strange parton distributions is illustrated by the comparison of the results obtained with the CTEQ5L [5](solid line) and GRV98LO [6](dashed line) parton distributions.

The GRV98 set is chosen because of its assumption that there is no intrinsic nucleon strangeness at a low scale and the strange sea is of pure perturbative origin. The CTEQ collaboration allows non-perturbative strangeness in the nucleon. The amount of this intrinsic strangeness is fixed from the dimuon data of the CCFR and NuTeV experiments [7]. As a result, the  $s(x)$  distribution of CTEQ is larger than the GRV98 one by a factor of about two in the region  $x = 0.001 - 0.01$ . The results in Fig. 3 show that the data on  $\Lambda$  can not discriminate between the predictions since the spin transfer to  $\Lambda$  is small. For the  $\bar{\Lambda}$  hyperon the use of CTEQ5L set leads to a prediction which is nearly twice larger than the one with the GRV98LO and much closer to the data. This behaviour reflects the difference in the corresponding  $\bar{s}$ -quark distributions.

If one switches off completely the spin transfer from the  $s(\bar{s})$  quarks, the spin transfer to  $\Lambda(\bar{\Lambda})$  practically vanishes (dash-dotted line). This feature is independent of the model of  $\Lambda$  spin structure. Calculations in the BJ-model [8], where the spin transfer from the  $u$ - and  $d$ -quarks(antiquarks) is possible, show the same absence of the spin transfer to hyperons without the contribution from the  $s(\bar{s})$ -quarks (dotted line).

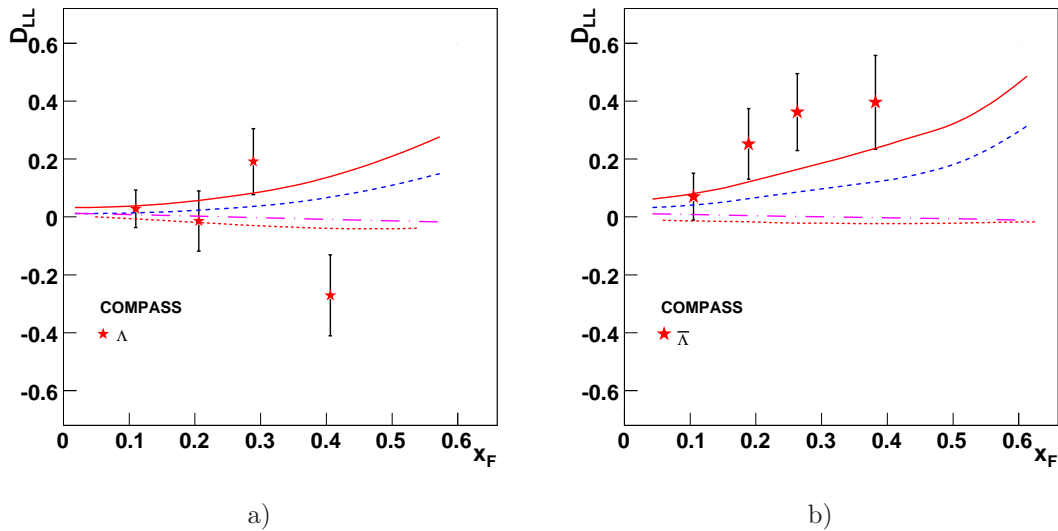


Figure 3: The  $x_F$  dependences of the longitudinal spin transfer to  $\Lambda$  (a) and  $\bar{\Lambda}$  (b) calculated in [3](model B) for the GRV98LO parton distribution functions (dashed lines), the CTEQ5L pdf (solid lines) and for the CTEQ5L without spin transfer from the  $s$ -quark (dash-dotted lines). The SU(6) model for the  $\Lambda$  spin structure is assumed. The dotted lines corresponds to the calculations for the CTEQ5L without spin transfer from the  $s$ -quark in the BJ-model of  $\Lambda$  spin [8].

At present the strange and antistrange quark distributions  $s(x)$  and  $\bar{s}(x)$  are directly accessible only through the measurement and study of dimuon events in neutrino and antineutrino DIS [9]. The spin transfer to  $\bar{\Lambda}$  could provide an additional experimental information to evaluate the strange quark distributions in the nucleon. To match this goal the present experimental precision must be increased and the theoretical uncertainties clarified.

The COMPASS data presented here are the most precise measurements to date of the longitudinal spin transfer to  $\Lambda$  and  $\bar{\Lambda}$  in DIS.

## References

- [1] Slides:  
<http://indico.cern.ch/contributionDisplay.py?contribId=295&sessionId=4&confId=53294>
- [2] COMPASS Collaboration, P.Abbon *et al.*, Nucl.Instr.Meth. **A577** 455 (2007).
- [3] J. Ellis, A.M. Kotzinian, D. Naumov, M.G. Sapozhnikov, Eur.Phys.J. **C52** 283 (2007).
- [4] Liang Zuo-tang *et al.*, arXiv:hep-ph/0902.1883 (2009).
- [5] F. Olness *et al.*, Eur.Phys.J. **C 40** 145 (2005).
- [6] M. Gluck, E. Reya, A. Vogt, Eur. Phys. J. **C5** 461 (1998).
- [7] CCFR and NuTeV Collaborations, M.Goncharov *et al.*, Phys.Rev. **D64** 112006 (2001).
- [8] M. Burkardt, R. L. Jaffe, Phys. Rev. Lett. **70** 2537 (1993).
- [9] D. Mason *et al.*, Phys.Rev.Lett. **99** 192001 (2007).